Research Square

Preprints are preliminary reports that have not undergone peer review.
They should not be considered conclusive, used to inform clinical practice,
or referenced by the media as validated information.

Development and Internal Validation of a Simplified Non-Contrast MRI Risk Model for Preoperative Differentiation of Ovarian Tumors

Mukhayo Khayitboeva
khayitboyeva@list.ru
Tashkent State Medical University
Marat Khodjibekov
Tashkent State Medical University
Madina Tairova
Tashkent State Medical University
Gulbakhor Khodjamova
Tashkent State Medical University
Uktam Kurbankulov
Tashkent State Medical University
Mukhabbat Djurabaeva
Tashkent State Medical University
Zilola Mirtadjieva
Treatment and Preventive Care Center under the Federation Council of Trade Unions of the Republic of Uzbekistan

Research Article

Keywords: ovarian tumors, ovarian cancer, magnetic resonance imaging, non-contrast MRI, adnexal masses, logistic regression, predictive model, diagnostic accuracy, risk stratification, O-RADS MRI

Posted Date: July 27th, 2026

DOI: https://doi.org/10.21203/rs.3.rs-10376173/v1

License: This work is licensed under a Creative Commons Attribution 4.0 International License.
Read Full License

Additional Declarations: No competing interests reported.

Development and Internal Validation of a Simplified Non-Contrast MRI Risk Model for Preoperative Differentiation of Ovarian Tumors

Mukhayo Khayitboeva[1]*, Marat Khodjibekov[1], Madina Tairova[1], Gulbakhor Khodjamova, Uktam Kurbankulov[1], Mukhabbat Djurabaeva[1], Zilola Mirtadjieva[2]

[1] Tashkent State Medical University, Tashkent, Uzbekistan
[2] Treatment and Preventive Care Center under the Federation Council of Trade Unions of the Republic of Uzbekistan, Tashkent, Uzbekistan
*Corresponding author: Mukhayo Khayitboeva
Tashkent State Medical University
Tashkent, Uzbekistan
Email: khayitboyeva@list.ru

Abstract

Background

Accurate preoperative differentiation between benign and malignant ovarian tumors remains a major clinical challenge because treatment strategy and prognosis depend substantially on tumor biology. Although magnetic resonance imaging (MRI) plays an important role in the characterization of adnexal lesions, conventional visual assessment may be limited by overlapping imaging features and observer-dependent interpretation. In addition, contrast-enhanced MRI protocols are not always feasible because of limited availability or contraindications to contrast administration. This study aimed to develop and internally validate a simplified predictive model based exclusively on routinely assessable non-contrast MRI features for preoperative differentiation of ovarian tumors.

Methods

This retrospective single-center study included 179 women with ovarian tumors who underwent preoperative pelvic MRI and subsequent surgical treatment between 2020 and 2025. Patients were divided into a training cohort (n = 126) for model development and an internal validation cohort (n = 53). Conventional MRI features were assessed using a structured checklist and transformed into categorical variables. Histopathological examination served as the reference standard. A multivariable logistic regression model was developed using selected non-collinear predictors, and diagnostic performance was evaluated using receiver operating characteristic (ROC) analysis.

Results

Multivariable logistic regression identified five independent MRI predictors of malignancy: lesion shape, wall thickness, papillary projections, regional lymph node enlargement, and pelvic fluid. In the training cohort, the model demonstrated excellent diagnostic performance with an area under the ROC curve (AUC) of 0.942 (95% CI: 0.885–0.976), sensitivity of 94.4%, specificity of 81.8%, and overall diagnostic accuracy of 87.9%. Internal validation demonstrated sensitivity of 70.6%, specificity of 89.5%, and overall accuracy of 77.4%, indicating acceptable reproducibility.

Conclusions

The proposed non-contrast MRI-based logistic regression model demonstrated effective differentiation between benign and malignant ovarian tumors using routinely assessable imaging features. The model may serve as an interpretable decision-support tool for preoperative risk stratification, particularly in settings where contrast-enhanced MRI is unavailable or contraindicated. Further external multicenter validation is required to confirm its generalizability and clinical utility.

Keywords: ovarian tumors; ovarian cancer; magnetic resonance imaging; non-contrast MRI; adnexal masses; logistic regression; predictive model; diagnostic accuracy; risk stratification; O-RADS MRI.

Introduction

Ovarian cancer is one of the leading causes of cancer-related mortality among women worldwide because it is frequently diagnosed at advanced stages due to the absence of specific early symptoms [1].

Similar diagnostic challenges are observed in low- and middle-income settings, where access to advanced imaging protocols may be limited. The primary clinical challenge in the evaluation of ovarian masses is differentiation between benign and malignant lesions, as treatment strategy and prognosis depend largely on tumor biology. Histopathological examination remains the diagnostic gold standard; however, preoperative biopsy of ovarian tumors is rarely performed because of technical limitations and the risk of tumor dissemination. Consequently, definitive diagnosis is often established only after surgical intervention, potentially leading to unnecessary invasive procedures.

Magnetic resonance imaging (MRI) is considered one of the most effective noninvasive imaging modalities for characterization of ovarian tumors because of its superior soft tissue contrast and high diagnostic performance in the assessment of adnexal lesions [6–8]. In routine clinical practice, MRI findings are predominantly interpreted using qualitative visual assessment, which is highly dependent on radiologist experience. In addition, imaging features of benign and malignant ovarian tumors frequently overlap, contributing to diagnostic uncertainty [7,9].

Previous studies comparing MRI findings with histopathological results have reported diagnostic accuracies ranging from 83% to 93% [8–10]. To improve diagnostic consistency and standardization of image interpretation, several MRI-based scoring systems have been developed, including the ADNEX MR scoring model and the standardized O-RADS MRI classification system [1,2,11,12]. These approaches have demonstrated high diagnostic performance and reproducibility; however, they generally require dynamic contrast-enhanced MRI, which may not be available or feasible in all clinical settings [2,6]. In addition, standardized MRI reporting terminology and lexicons have been developed to improve consistency and reproducibility in the description of adnexal lesions across institutions and readers [16].

Despite improved standardization, MRI interpretation remains partially dependent on radiologist expertise, and indeterminate lesions continue to represent

a diagnostic challenge even within standardized MRI classification systems such as O-RADS MRI [3,11–14].

In routine clinical practice, contrast-enhanced MRI cannot always be performed because of limited availability, prolonged examination protocols, economic considerations, or contraindications to gadolinium-based contrast agents. Therefore, simplified non-contrast MRI approaches that rely on routinely assessable morphological features may provide a practical alternative for preoperative risk assessment [4,10,17,18].

Therefore, this study aimed to develop and internally validate an interpretable logistic regression model based exclusively on routinely assessable non-contrast MRI features as a decision-support tool for preoperative risk stratification of ovarian tumors.

Materials and Methods

Study Design and Patients

This retrospective single-center study included 179 female patients aged 20–72 years with ovarian tumors who underwent preoperative pelvic MRI examination and subsequent surgical treatment at the Republican Specialized Scientific and Practical Medical Center of Oncology and Radiology of the Republic of Uzbekistan between 2020 and 2025.

The study population was divided into two independent cohorts:

(1) a training cohort consisting of 126 patients used for predictive model development and

(2) an internal hold-out validation cohort consisting of 53 patients used for validation of model performance.

In the internal hold-out validation cohort, histopathological examination identified benign ovarian tumors in 19 patients and malignant ovarian tumors in 34 patients.

All patients underwent surgical treatment. Diagnostic laparotomy was performed in 12 patients. Laparoscopic hysterectomy with bilateral salpingo-oophorectomy and omentectomy was performed in 15 patients. The remaining 99 patients underwent laparotomy with hysterectomy, bilateral salpingo-oophorectomy, and omentectomy.

In all cases, tumor tissue samples were obtained for histopathological examination, which served as the reference standard.

Preoperative serum CA-125 levels were measured in all patients.

According to histopathological findings in the training cohort, 54 patients (42.8%) had benign ovarian tumors and 72 patients (57.1%) had malignant ovarian tumors. The histopathological distribution of ovarian tumors in the training cohort is presented in Table 1.

Table 1. Histopathological distribution of ovarian tumors in the training cohort (n = 126)

Tumor category	Histological type	n (%)
Benign ovarian tumors (n = 54, 42.8%)	Serous cystadenoma	27 (50.0)
	Endometriotic cyst	10 (18.5)

	Hemorrhagic cyst	7 (13.0)
	Mucinous cystadenoma	4 (7.4)
	Follicular cyst	5 (9.3)
	Dermoid cyst	1 (1.8)
Malignant ovarian tumors (n = 72, 57.1%)	Serous adenocarcinoma	45 (62.5)
	Mucinous adenocarcinoma	2 (2.8)
	Dysgerminoma	14 (19.4)
	Granulosa cell tumor	7 (9.7)
	Borderline Brenner tumor	4 (5.6)

Outcome Definition

The reference standard for outcome classification was postoperative histopathological examination. Ovarian lesions were categorized into benign and malignant groups according to final histopathological diagnosis. Borderline tumors were included in the malignant outcome category because they were managed according to oncologic treatment protocols and their small number precluded separate subgroup analysis.

Clinical Characteristics

Patient age ranged from 20 to 72 years. Benign ovarian tumors were more frequently observed in patients aged 20–40 years (51.8%), whereas malignant tumors predominantly occurred in patients older than 40 years (80.6%).

Tumor grading was available in 38 patients with malignant ovarian tumors. Well-differentiated tumors (G1) were identified in 15 patients, moderately differentiated tumors (G2) in 12 patients, and poorly differentiated tumors (G3) in 11 patients.

Tumor staging was performed according to the International Federation of Gynecology and Obstetrics (FIGO) classification system (Table 2). Most malignant ovarian tumors were diagnosed at advanced stages (FIGO III–IV).

Table 2. Distribution of patients according to the FIGO staging system for ovarian cancer

FIGO stage	Number of patients (n)	%
I–IIA	24	33.3
IIB–III–IV	40	55.5
X (unknown / not assessed)	8	11.1

Most patients with malignant ovarian tumors were diagnosed at advanced stages (FIGO III–IV). In eight patients, insufficient data were available for accurate staging.

MRI Acquisition

Pelvic MRI examinations were performed using a 1.5-T MRI scanner (Magnetom Sonata; Siemens Healthcare, Erlangen, Germany). Prior to imaging, all

patients underwent standard preparation aimed at reducing bowel peristalsis artifacts, including adherence to a low-fiber diet for two days before MRI acquisition.

The MRI protocol included high-resolution T2-weighted images acquired in axial, sagittal, and coronal planes using turbo spin-echo (TSE), fast spin-echo (FSE), and rapid acquisition with relaxation enhancement (RARE) sequences. T1-weighted spin-echo images were obtained with and without fat suppression. Diffusion-weighted imaging (DWI) was performed using echo-planar imaging sequences with fat suppression.

No intravenous contrast agents were administered.

MRI Feature Assessment

MRI examinations were analyzed using a structured checklist of predefined imaging features (Table 3).

Table 3. Structured MRI checklist for assessment of ovarian lesions

No.	MRI feature	Categories
1	Lesion size	≤6 cm / >6 cm
2	Lesion shape	Regular / Irregular
3	Laterality	Unilateral / Bilateral
4	Lesion margins	Well-defined / Ill-defined
5	Lesion type	Cystic / Cystic–solid / Predominantly solid
6	Wall thickness of cystic lesions	Normal (≤3 mm) / Thickened (>3 mm)
7	Inner wall surface of cystic lesion	Smooth / Irregular
8	Papillary projections of walls or septa	Absent / Present
9	Size of papillary projections	≤3 mm / >3 mm
10	Ascites	Absent / Present
11	Excess pelvic fluid	Absent / Present
12	Peritoneal metastases	Absent / Present
13	Regional lymph node size	Normal (≤10 mm) / Enlarged (>10 mm)
14	Menopausal status	Premenopausal / Postmenopausal
15	CA-125 level	≤35 U/mL / >35 U/mL

The evaluated MRI features included lesion size, shape, laterality, lesion margins, lesion composition, wall thickness, inner wall irregularity, presence and size of papillary projections, ascites, pelvic fluid, peritoneal metastases, regional lymph node enlargement, menopausal status, and serum CA-125 level.

Predictor Selection

Candidate predictors were selected based on clinical relevance and previous literature. Variables demonstrating multicollinearity were excluded before model fitting.

Predictive Model Development

A supervised predictive modeling approach based on multivariable logistic regression analysis was used to differentiate benign and malignant ovarian tumors using conventional non-contrast MRI features.

The model development process consisted of several sequential steps. Initially, visually assessed MRI features were converted into categorical variables using a predefined scoring system. An experienced radiologist performed categorical assessment of MRI characteristics using standardized imaging criteria.

Prior to predictive model construction, MRI features were categorized using predefined binary scoring criteria. For example, lesion size ≤60 mm was assigned a score of 0, whereas lesion size >60 mm was assigned a score of 1. Smooth lesion margins were scored as 0, while irregular margins were scored as 1. The absence of ascites was scored as 0, whereas its presence was scored as 1.

The categorized MRI variables were subsequently entered into a computerized dataset for predictive model development. Variables associated with malignancy in univariable analysis were entered into multivariable logistic regression.

Based on the selected non-collinear predictors, a multivariable logistic regression model was constructed using training cohort data.

Model discrimination ability was evaluated using receiver operating characteristic (ROC) curve analysis. The optimal discrimination threshold for classification of ovarian lesions was determined using the Youden index.

Validation of the Predictive Model

Validation of the predictive model was performed using an independent test cohort consisting of 53 patients with ovarian tumors.

For each patient in the test cohort, the MRI malignancy index was calculated using the logistic regression equation developed on the training cohort data. Classification performance was assessed using the predefined discrimination threshold (>0.3062).

Sensitivity, specificity, and overall diagnostic accuracy obtained in the test cohort were compared with those observed in the training cohort to evaluate model reproducibility and generalizability.

Statistical Analysis

Statistical analysis was performed using MedCalc (MedCalc Software Ltd, Ostend, Belgium).

Continuous variables were summarized as mean ± standard deviation or median (interquartile range), depending on distribution.

Categorical variables were presented as frequencies and percentages.

Differences between benign and malignant groups were evaluated using the chi-square test or Fisher exact test for categorical variables and Student’s t-test or Mann–Whitney U test for continuous variables, as appropriate.

Candidate MRI predictors were assessed for multicollinearity prior to model construction.

Multivariable logistic regression analysis with backward stepwise selection was used to develop the predictive model.

Model discrimination was assessed using ROC analysis and area under the curve (AUC).

Diagnostic performance was evaluated using sensitivity, specificity, overall accuracy, positive predictive value, and negative predictive value.

Statistical significance was defined as $p < 0.05$.

Ethics Approval and Consent to Participate

The study was conducted in accordance with the principles of the Declaration of Helsinki. The study protocol was approved by the local Ethics Committee of the Republican Specialized Scientific and Practical Medical Center of Oncology and Radiology (Uzbekistan).

Written informed consent was obtained from all patients prior to inclusion in the study.

Results

Based on the visual assessment of conventional MRI images, three types of ovarian tumor MRI patterns were identified:

- **Type 1**: unilocular or multilocular cystic lesions with thin (≤3 mm) and smooth walls;
- **Type 2**: cystic lesions with large papillary projections (>3 mm) and a solid component;
- **Type 3**: predominantly solid lesions.

The distribution of lesions according to MRI pattern types is presented in **Table 4**.

Table 4. Histological types of ovarian tumors and their frequency according to MRI pattern types.

MRI pattern type	Histological type of ovarian tumor	Number of patients	%
Unilocular and multilocular cystic lesions without or with single small papillary projections (≤3 mm) (n = 49)	Follicular cyst	5	10.2
	Serous cystadenoma	18	36.7
	Mucinous cystadenoma	4	8.2
	Endometriotic cyst	10	20.4
	Hemorrhagic cyst	7	14.3
	Serous adenocarcinoma	5	10.2
Cystic lesions with large papillary projections (>3 mm) and solid component (n = 51)	Serous cystadenoma	9	17.6
	Serous adenocarcinoma	40	78.4
	Mucinous adenocarcinoma	2	4.0

MRI pattern type	Histological type of ovarian tumor	Number of patients	%
Predominantly solid lesions (n = 26)	Dermoid cyst	1	3.8
	Dysgerminoma	14	53.8
	Granulosa cell tumor	7	26.9
	Brenner tumor	4	15.4

Benign ovarian tumors predominantly demonstrated unilocular or multilocular thin-walled cystic morphology with smooth margins and homogeneous high T2-weighted signal intensity (Figure 1). Mucinous cystadenomas frequently demonstrated heterogeneous internal signal intensity ("stained glass" appearance) (Figure 2), whereas endometriotic cysts showed characteristic T1 hyperintensity with T2 shading (Figure 3).

Malignant ovarian tumors more frequently demonstrated cystic-solid or predominantly solid morphology, irregular margins, thickened septa, papillary projections, ascites, and regional lymph node enlargement (Table 5). Representative examples of malignant ovarian tumors are shown in Figures 4–7.

Table 5. Frequency of MRI features suggestive of malignancy in benign and malignant ovarian tumors (n, %)

MRI feature	Benign tumors (n = 54)	Malignant tumors (n = 72)
Irregular lesion shape	18 (33.3%)	52 (72.2%)
Cystic–solid or predominantly solid lesion	11 (20.4%)	65 (90.3%)
Ill-defined lesion margins	0 (0%)	44 (61.1%)
Thickened walls/septa (>3 mm)	6 (11.1%)	44 (61.1%)
Irregular inner wall surface	25 (46.3%)	58 (80.6%)
Presence of papillary projections	9 (16.7%)	40 (55.6%)
Large papillary projections (>3 mm)	2 (3.7%)	34 (47.2%)
Signal intensity ratio of solid component to myometrium (<1.5)	12 (22.7%)	46 (63.9%)
Enlarged regional lymph nodes (>10 mm short axis)	5 (9.2%)	36 (50.0%)
Peritoneal metastases	0 (0%)	40 (55.6%)
Ascites	3 (5.6%)	42 (58.4%)
Excessive fluid in the Douglas pouch	3 (5.6%)	28 (38.9%)
Diffusion restriction on DWI	4 (7.4%)	26 (36.1%)

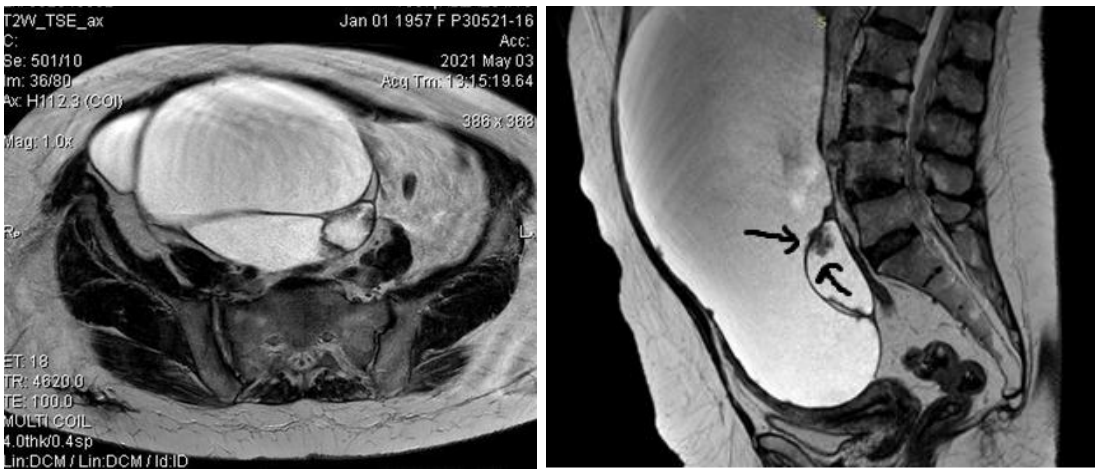


Figure 1. Serous cystadenoma of the left ovary. Axial and sagittal T2-weighted images demonstrate a multilocular cystic lesion with smooth walls and a small papillary projection (arrows).

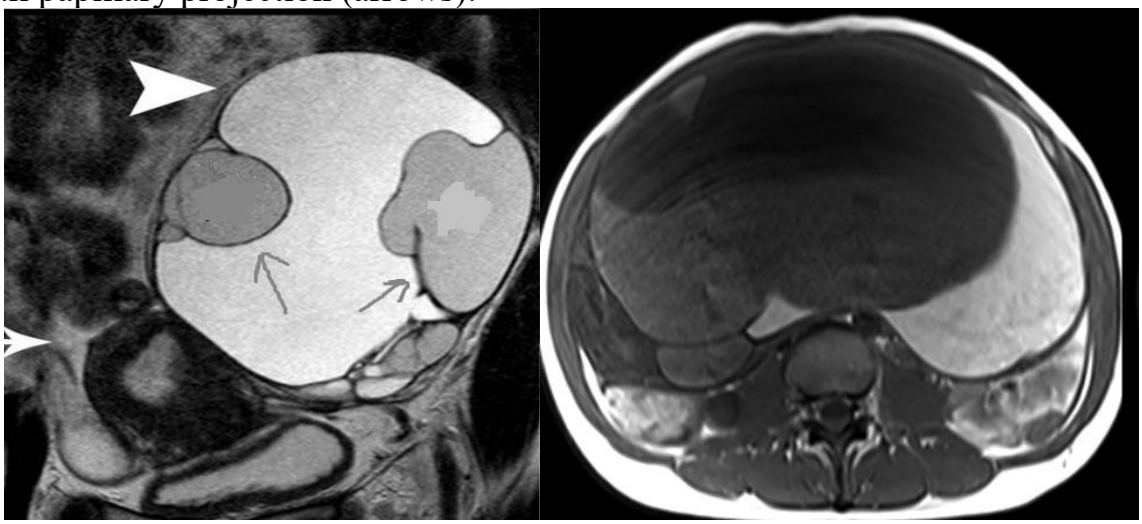


Figure 2. Mucinous cystadenoma of the ovary demonstrating heterogeneous internal signal intensity ("stained glass" appearance).

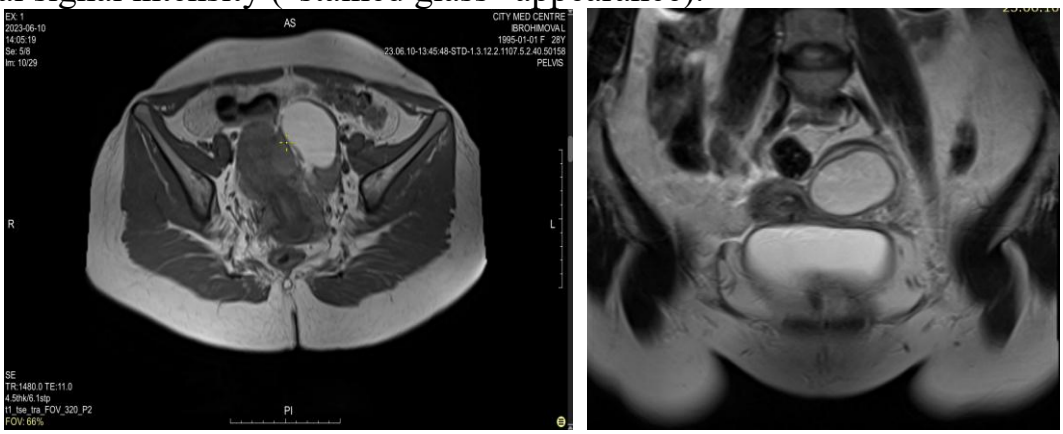


Figure 3. Endometriotic cyst demonstrating T1 hyperintensity with characteristic T2 shading.



Figure 4. Hemorrhagic ovarian cyst demonstrating heterogeneous internal signal intensity.



Figure 5. Serous cystadenocarcinoma demonstrating multilocular cystic-solid morphology with papillary projections.

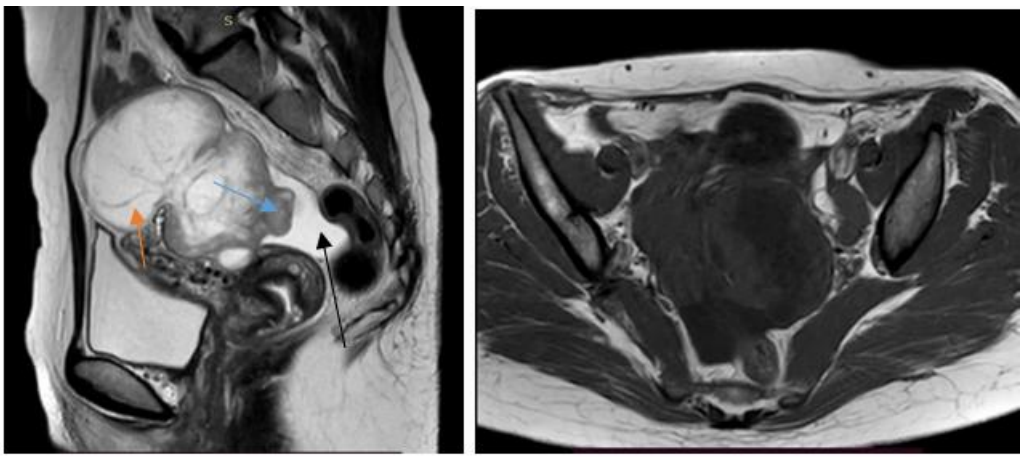


Figure 6. Bilateral serous cystadenocarcinoma with thickened walls and papillary projections.

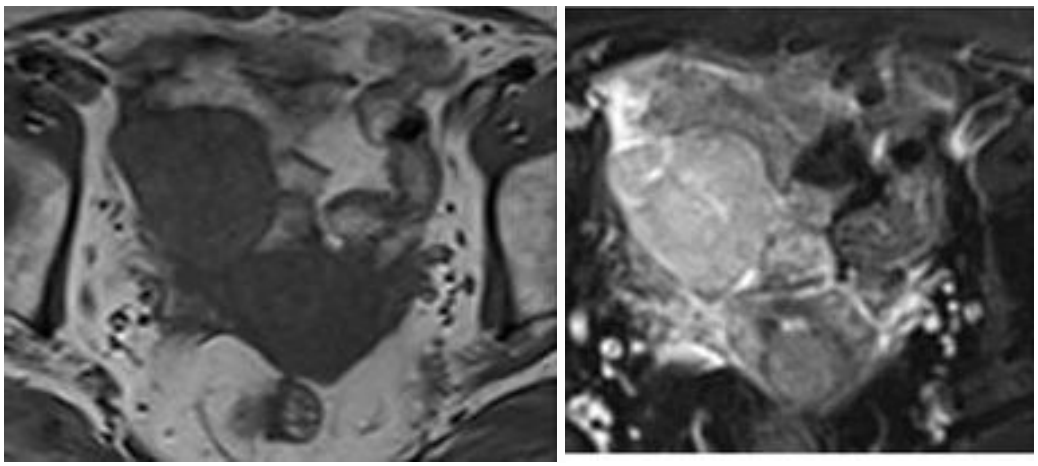


Figure 7. Granulosa cell tumor demonstrating predominantly solid morphology.

Relevant MRI features associated with tumor malignancy were identified using the Kruskal–Wallis test (Table 6).

Table 6. Statistical significance of MRI features for predicting ovarian tumor malignancy (Kruskal–Wallis test)

No.	MRI feature	H value	p value
1	Lesion size >60 mm	3.548	0.06*
2	Bilateral involvement	2.634	0.105*
3	Irregular lesion shape	18.2	<0.001
4	MRI pattern types III–IV	68.5	<0.001
5	Ill-defined lesion margins	50.3	<0.001
6	Wall/septal thickness >3 mm	28.2	<0.001
7	Irregular inner wall surface	15.9	<0.001
8	Presence of papillary projections	18.2	<0.001
9	Papillary projection size >3 mm	25.1	<0.001
10	Signal intensity ratio (solid component / myometrium) on T2WI	23.1	<0.001
11	Regional lymph nodes >10 mm	15.2	<0.001
12	Peritoneal metastases	43.6	<0.001
13	Ascites	37.1	<0.001
14	Excessive fluid in the Douglas pouch	18.3	<0.001
15	Diffusion restriction on DWI	10.0	0.002

Significant differences were observed for 13 of the 15 evaluated MRI features, indicating their relevance for malignancy prediction.

Multivariable logistic regression analysis identified five independent non-collinear MRI predictors of malignancy:

1. Lesion shape;

2. Wall thickness;
3. Presence of papillary projections;
4. Size of regional lymph nodes;
5. Presence of pelvic fluid.

The adequacy of the selected predictors was confirmed by Wald statistics (Table 7).

Table 7. Wald test results for independent predictors in the MRI-based logistic regression model

Predictor variable	Wald statistic	p value
Wall thickness	16.944	0.0001
Regional lymph node size	8.1339	0.0043
Lesion shape	10.0472	0.0015
Papillary projections	11.7423	0.0006
Fluid in the Douglas pouch	8.6134	0.0033
Constant	21.4306	<0.0001

Using these variables, a logistic regression model for predicting the histological nature of ovarian tumors was developed:

$Y = 1 / [1 + \exp - (-4.46856 + 3.09234x_1 + 2.00053x_2 + 2.37226x_3 + 1.27840x_4 + 2.53123x_5)]$, where *Y* represents the malignancy index;

x_1 wall thickness;

x_2 lymph node size;

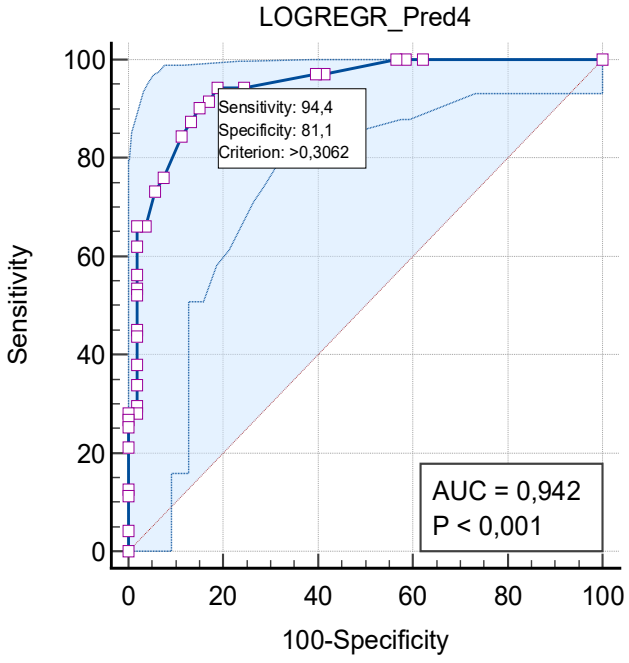
x_3 lesion shape;

x_4 papillary projections;

x_5 presence of pelvic fluid.

Model performance was evaluated using ROC analysis (Figure 8).

Figure 8. Receiver operating characteristic (ROC) curve of the MRI-based logistic regression model for predicting the nature of ovarian lesions.



The selected discrimination threshold was chosen to optimize overall diagnostic performance and was subsequently used for validation analysis.

The area under the ROC curve was 0.942 ± 0.022 ($p < 0.001$), with a 95% confidence interval of 0.885–0.976. Sensitivity was 94.4%, specificity 81.1%, overall accuracy 87.9%, positive predictive value 94.7%, and negative predictive value 75.0%, with an optimal discrimination threshold of >0.3062.

Validation of the Predictive Model

The predictive performance of the MRI-based logistic regression model was additionally evaluated using an internal hold-out validation cohort consisting of 53 patients with ovarian tumors. For each patient, the malignancy index was calculated using the regression equation derived from the training cohort data (n = 126). Lesions were classified as benign or malignant according to the predefined discrimination threshold of >0.3062.

In the validation cohort, histopathological examination identified benign ovarian tumors in 19 patients and malignant ovarian tumors in 34 patients. The MRI-based predictive model demonstrated a sensitivity of 70.6%, specificity of 89.5%, and overall diagnostic accuracy of 77.4%. In comparison, the corresponding diagnostic performance values in the training cohort were 94.4%, 81.8%, and 87.9%, respectively (Table 8).

Table 8. Comparison of diagnostic performance of the MRI-based malignancy index between the training and validation cohorts.

Cohort	Number of patients	Sensitivity (%)	Specificity (%)	Accuracy (%)
Training cohort	126	94.4	81.8	87.9
Validation cohort	53	70.6	89.5	77.4

Comparative analysis demonstrated no statistically significant differences in specificity and overall diagnostic accuracy between the training and validation cohorts ($p > 0.05$), indicating acceptable reproducibility of the proposed predictive model. However, sensitivity was lower in the validation cohort. In the validation cohort, sensitivity was lower than in the training cohort, whereas specificity and overall diagnostic accuracy remained relatively stable. This observation may reflect differences in case distribution between cohorts and emphasizes the need for further external validation in larger patient populations.

Discussion

Conventional MRI remains an important imaging modality for preoperative characterization of ovarian tumors because of its high soft tissue contrast and ability to depict morphologic features associated with malignancy. However, differentiation between benign and malignant ovarian lesions continues to be challenging due to overlapping imaging appearances and variability in image interpretation.

In the present study, we developed and internally validated an interpretable logistic regression model based exclusively on routinely assessable non-contrast

MRI features for differentiation of benign and malignant ovarian tumors. The proposed model demonstrated high discrimination ability in the training cohort and maintained reasonable diagnostic performance in the validation cohort, supporting its potential role as a decision-support tool for preoperative risk stratification.

Previous studies have shown that MRI-based scoring systems may improve standardization and diagnostic reproducibility in the assessment of adnexal lesions. Established approaches such as the O-RADS MRI classification system have demonstrated high diagnostic performance and contributed to more structured interpretation of ovarian lesions. However, these approaches frequently rely on contrast-enhanced imaging protocols and structured interpretation workflows. Recent multicenter investigations have further confirmed the high diagnostic performance of the O-RADS MRI scoring system for characterization of adnexal masses, supporting its role in standardized MRI assessment of ovarian lesions [5].

The present model was not designed to replace established MRI classification systems but rather to provide an alternative decision-support approach in situations where contrast-enhanced MRI is unavailable, impractical, or contraindicated. In this context, simplified non-contrast MRI assessment may represent a clinically applicable strategy for preoperative risk stratification.

An important strength of the proposed model is that all predictors were derived from routinely assessable conventional MRI features without administration of contrast agents. The final model included lesion shape, wall thickness, papillary projections, regional lymph node enlargement, and pelvic fluid, all of which demonstrated independent association with malignancy. Selection of a limited number of predictors allowed development of an interpretable model while reducing complexity and maintaining diagnostic performance.

The diagnostic performance observed in the training cohort demonstrated high sensitivity and acceptable specificity. During validation, sensitivity decreased whereas specificity and overall diagnostic performance remained relatively stable. This finding may reflect differences in case distribution between cohorts and emphasizes the importance of future external validation in larger patient populations.

Compared with visual MRI assessment alone, the proposed model may contribute to more standardized risk estimation and support radiologists in situations characterized by diagnostic uncertainty. Nevertheless, interpretation of ovarian MRI findings remains dependent on imaging quality, reader experience, and clinical context.

This study has several limitations. First, the study had a retrospective single-center design, which may limit generalizability of the findings. Second, the validation cohort was relatively small and included heterogeneous histological subtypes of ovarian tumors. Third, MRI feature assessment was based on manually categorized imaging characteristics, which may introduce observer-dependent variability. Finally, model performance was evaluated using internal hold-out validation rather than external multicenter validation.

Therefore, the proposed model should be considered as a decision-support tool rather than a replacement for established MRI classification systems. Future studies should focus on external validation and assessment of clinical utility across different patient populations.

Conclusions

The proposed MRI-based logistic regression model, when used in addition to conventional visual MRI assessment, demonstrated effective differentiation between benign and malignant ovarian lesions, achieving an overall diagnostic accuracy of 87.9% in the training cohort.

Based exclusively on routinely assessable non-contrast MRI features, the model may serve as a decision-support tool for preoperative risk stratification of ovarian tumors, particularly in settings where contrast-enhanced MRI is unavailable or contraindicated.

Further external multicenter validation studies with larger patient populations are required to confirm the reproducibility, generalizability, and potential clinical utility of the proposed model.

Declarations

Clinical trial number

Not applicable

Ethics approval and consent to participate

The study was approved by the Ethics Committee of Tashkent State Medical University and was conducted in accordance with the Declaration of Helsinki. Due to the retrospective observational design of the study and the use of anonymized clinical and imaging data, the requirement for informed consent was waived by the Ethics Committee.

Human Ethics and Consent to Participate declarations

The study involved human participants and was approved by the Ethics Committee of Tashkent State Medical University. The study was conducted in accordance with the Declaration of Helsinki. Due to the retrospective observational design and use of anonymized data, the requirement for informed consent was waived by the Ethics Committee.

Consent for publication

Not applicable.

Availability of data and materials

The datasets generated and/or analyzed during the current study are not publicly available due to institutional and ethical restrictions related to patient confidentiality but are available from the corresponding author on reasonable request.

Competing interests

The authors declare that they have no competing interests.

Funding

The authors received no specific funding for this study.

Authors' contributions

M.Kh. conceived and designed the study.

M.Kh., M.H., and M.T. collected the clinical and MRI data.

G.Kh. and U.K. performed MRI interpretation and image analysis.
M.D. performed the statistical analysis.
Z.M. contributed to data interpretation and manuscript revision.
M.Kh. drafted the manuscript.
All authors critically revised the manuscript and approved the final version.

Acknowledgements
Not applicable.

References

1. Thomassin-Naggara I, Poncelet E, Jalaguier-Coudray A, et al. O-RADS MRI score for risk stratification of sonographically indeterminate adnexal masses. JAMA Netw Open. 2020;3(1):e1919896.

2. Sadowski EA, Thomassin-Naggara I, Rockall A, et al. O-RADS MRI risk stratification system: guide for assessing adnexal lesions from the ACR O-RADS Committee. Radiology. 2022;303(1):35–47.

3. Koch C, Kinkel K, Forstner R, et al. O-RADS MRI: practical implementation and reader experience requirements. Insights Imaging. 2023;14(1):1–12.

4. Sahin H, Yildirim D, Akyol M, et al. Diagnostic performance of a non-contrast-enhanced O-RADS MRI scoring system for adnexal masses. Eur J Radiol. 2021;144:109964.

5. Dabi Y, Thomassin-Naggara I, Bazot M, et al. Diagnostic performance of O-RADS MRI scoring system for adnexal masses: a multicenter study. Eur Radiol. 2024;34(2):1012–1021.

6. Forstner R, Thomassin-Naggara I, Cunha TM, et al. ESUR recommendations for MR imaging of the sonographically indeterminate adnexal mass: an update. Eur Radiol. 2017;27(6):2248–2257.

7. Thomassin-Naggara I, Aubert E, Rockall A, et al. Adnexal masses: development and preliminary validation of an MR imaging scoring system. Radiology. 2013;267(2):432–443.

8. Ruiz M, Labauge P, Louboutin A, et al. External validation of the MR imaging scoring system for the management of adnexal masses. Eur J Obstet Gynecol Reprod Biol. 2016;205:115–119.

9. Sasaguri K, Yamaguchi K, Nakazono T, et al. External validation of ADNEX MR scoring system: a single-center retrospective study. Clin Radiol. 2019;74(2):131–139.

10. Pereira PN, Sarian LO, Yoshida A, et al. Accuracy of the ADNEX MR scoring system based on a simplified MRI protocol for the assessment of adnexal masses. Diagn Interv Radiol. 2018;24(2):63–71.

11. Rizzo S, Manganaro L, Testa AC, et al. O-RADS MRI: a systematic review and meta-analysis of diagnostic performance for adnexal lesion characterization. Radiology. 2022;305(2):265–278.

12. Thomassin-Naggara I, Belghiti J, Milon A, et al. O-RADS MRI score: analysis of misclassified cases in a prospective multicenter European cohort. Eur Radiol. 2021;31(12):9588–9599.

13. Sadowski EA, Thomassin-Naggara I, Rockall A, et al. O-RADS MRI after initial ultrasound for adnexal lesions. AJR Am J Roentgenol. 2023;221(2):250–259.

14. Nougaret S, Thomassin-Naggara I, Rockall A, et al. O-RADS MRI risk stratification system: pearls and pitfalls. Insights Imaging. 2024;15(1):45.

15. Andreotti RF, Timmerman D, Strachowski LM, et al. O-RADS US risk stratification and management system: a consensus guideline from the ACR O-RADS Committee. Radiology. 2020;294(1):168–185.

16. Reinhold C, Rockall A, Sadowski EA, et al. Ovarian-adnexal reporting lexicon for MRI: a white paper of the ACR O-RADS MRI Committee. J Am Coll Radiol. 2021;18(5):713–729.

17. Ramalto O, Le Fur Y, Gandon Y. Gadolinium-based contrast agents: risk of tissue retention and nephrogenic systemic fibrosis. Diagn Interv Imaging. 2016;97(6):583–589.

18. The Royal College of Radiologists. Standards for intravascular contrast agent administration to adult patients. London: RCR; 2019.